Journal of Applied Fluid Mechanics, Vol. 16, No. 4, pp. 794-804, 2023.
Available online at www.jafmonline.net, ISSN 1735-3572, EISSN 1735-3645.
https://doi.org/10.47176/jafm.16.04.1475

Flow Field Investigation of a Blended Wing Body in Low Speeds

A. Arora, S. Das and P. Kumar†

Department of Space Engineering & Rocketry, BIT, Ranchi, Jharkhand, -835215, India

†*Corresponding Author Email: priyankkumar@bitmesra.ac.in*

(Received August 23, 2022; accepted November 22, 2022)

ABSTRACT

With the advancement in the modern transport system, it has become imperative to achieve larger aircraft volume at minimum cost wherein aerodynamics plays a major role. The present work aims to investigate the flow over a typical blended wing body (BWB) configuration at different angles of attack adopting experimental and computational techniques. Experiments consisted of the force measurements and oil flow visualizations at a free stream velocity of around 19 m/s. Computations were made using the commercially available software ANSYS 18.1. Results indicated that the use of a Blended Wing Body Configuration resulted in improved aerodynamic characteristics in comparison to other wing configurations such as Delta/ Double delta wings. Surface flow visualization carried out over the BWB configuration indicated the reason behind increased lift coefficients. Reasonable agreement of experiments and computations was observed.

Keywords: Blended wing body; Oil flow; Experiment; UAV.

NOMENCLATURE

C_D	coefficient of drag
CFD	Computational Fluid Dynamics
C_L	coefficient of lift
L/D	lift to drag ratio
LUAV	Unmanned Aerial Vehicle
x/C	non-dimensional distance along root chord
α	angle of attack
ρ	density of air

1. Introduction

In the modern aerospace industry, an optimized aircraft configuration is required which can meet the demands of transportation, defence, and other related applications. Improvement is required in the efficiency, payload capacity, versatility, reduced emissions and noise, improved affordability, and others. Aerodynamics can be one of the key factors which can be used in resolving the mentioned concerns. Aerodynamic design and modifications will be required to reduce the vortex, wave, pressure and friction drag, thereby improving the load-carrying capacity and efficiency. The Blended Wing Body configuration is a possible answer for the above-mentioned issues and hence it is important to explore the flow physics over a BWB. It is expected that, unlike the delta/ double delta wing,

the flow over BWB will remain attached even at higher angles of attack, contributing towards increased lift, reduced drag, and better stability. There are several aircraft that have incorporated some aspects of a Blended Wing Body design, such as the B1-B Lancer and the B2 Bomber. This configuration can offer advantages in terms of aerodynamic efficiency, noise, and increased internal volume. For UAVs, the increase in aerodynamic efficiency, due to low wetted area, can offer advantages in terms of energy consumption which is a limiting factor for range and endurance. The increase in internal volume offers increased payload capacity improving the mission capabilities of UAVs. Figure 1 shows a typical flow over a blended wind body at angles of attack. The flow over a blended wing body appears to be attached which helps in the generation of the lift, like in the case of an aerofoil. While the shape of the BWB seems to be similar to the double delta wing, the flow physics at angles of attack is entirely different than the latter. Since the ratio of the internal volume to the surface area is quite larger in case of a BWB, it is important to investigate the overall flow physics existing on the vehicle. The possible factors affecting the flow field of the BWB are the geometrical shape, wing sweep, aerofoil section, Reynolds number, free stream velocity, and the angle of attack.

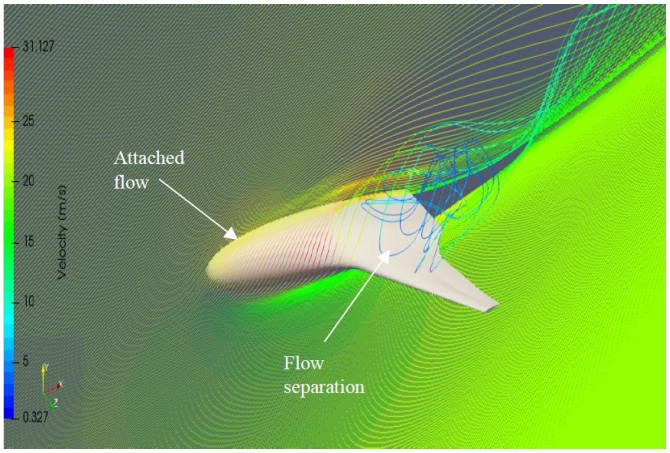

Fig. 1. Flow over a typical BWB model, Midhun *et al.* (2019).

In the past two decades, extensive works adopting experiments and computational methods have been done towards optimizing the shape of the Blended Wing Body. Qin *et al.* (2002) reported the aerodynamic aspect of BWB design with potential advantages it can offer over conventional designs. The major focus of the study was at high Mach numbers in the transonic range. Liebeck (2003, 2004) and Qin *et al.* (2004) formulated a BWB concept with complete design considerations of aerodynamics, structure, propulsion, stability, control, and other design aspects. The design procedure of an aircraft designated BWB-450 was also discussed and compared with conventional designs. Initial studies about the low noise aircraft, conducted by Hileman *et al.* (2007) reported considerations about a lifting body design and its efficiency. Siouris and Qin (2007) studied the effect of aerodynamic sweep on the aerodynamic performance of the BWB aircraft at a Mach number of 0.85 using computational methods. The study reported that the use of a wing sweep angle of 38 deg was observed to yield better aerodynamics efficiency in comparison to the other sweep angles, given structural concerns. Al-Garni *et al.* (2008) performed experiments and computational studies over a 65 deg delta wing and 65/40 degree double delta wing at different angles of attack. The wings had similar sweep angles to those studied by Qin *et al.* (2002, 2004) and the tests were performed at a lower Mach number. Kuntawala *et al.* (2011) carried out the optimization of the BWB model using a high fidelity, inviscid Euler-based solver at a Mach number of 0.85. Results indicated a 52% drag reduction. Other researchers namely Lehmkuehler *et al.* (2012), Lyu and Joaquim (2013a,b) and Dommelan and Roelof (2014) worked towards the optimization of the BWB shape using numerical techniques focussing on increasing the internal volume to accommodate passengers. Kashitani *et al.* (2015) conducted the experiments on a large sweep, reflex wing configuration BWB to obtain the aerodynamic characteristics in low-speed flows. The experiments were done at a free stream velocity of 25m/s and a Reynolds number of 2.6 x 10^5 based on the mean aerodynamic chord length. The wake integration method was used to obtain the aerodynamic characteristics with the help of a five-hole probe. Results indicated that a major amount of lift was generated at the mid-portion of the BWB because of its aerofoil shape. Larkina and Coates (2017) carried out computational studies over a BWB model with vertical stabilizers and reported that a twin-stabilizer configuration could be useful for the directional stability of the aircraft. A CFD analysis of BWB with 0 deg and 40 deg sweep angles was conducted by Panagiotou and Yakinthos (2017). Results indicated that the use of a 0 deg sweep angle was most suitable in the medium angle of attack range, however, the use of a 40 deg sweep angle delayed the stall and improved the stability. It was also concluded that a BWB configuration can be well utilized for the UAV applications in a low subsonic regime. Zeng *et al.* (2017) did the computational analysis on a typical BWB - Integrated Transitioning UAV (BITU) and indicated that BITU had high adaptability and survivability to varying wind conditions. Studies on the design optimizations of BWB were also reported by Panagiotou *et al.* (2018) and Brown and Vos (2018). Experimental analysis conducted by Yamada *et al.* (2019) in a low-speed tunnel at a free stream velocity of 18m/s indicated that the use of gurney flaps on the BWB configurations generated a pair of counter-rotating vortices and also improved the lift locally. Several BWBs under the prototyping stage are reported by Thompson *et al.* (2011), Becker and Sheffler (2016), Rodzewicz *et al.* (2018), Footohi *et al.* (2019), Naeini *et al.* (2019, 2021) and many others.

Literature indicates that the majority of studies pertaining to the Blended Wing Body have been done towards the optimization of the shape and evaluation of aerodynamic characteristics for different shapes adopting analytical and computational methods. Limited experimental works have been carried out to analyze the flow over the BWB shape and its impact on the aerodynamic characteristics. And hence it is imperative to investigate the flow over a Blended Wing Body and its superiority over the conventional aerofoil aircraft in terms of the aerodynamic efficiency at different angles of attack. The present investigations have been done at low speeds to understand the flow behaviour during take-off, landing and manoeuvring of a BWB which finds its applicability also towards the unmanned aerial vehicles.

2. METHODOLOGY

The present investigation focuses on the flow investigation over a BWB at different angles of attack and low speed adopting experiments and computational methods. Although a transport aircraft is supposed to fly at higher Mach numbers during its flight, the vehicle encounters low speeds and non – zero angle of attack during the time of take-off and landings. Even unmanned aerial vehicles do encounter a low speed during its flight. In the current scenario, one of the major requirement from defence perspective would be to carry more load with a minimum surface area and the use of a Blended Wing Body could be well suited in addressing these demands. In the current investigation, a typical model reported in Qin *et al.* (2004) has been considered which has root chord length of 188mm. The sweep angle for nose and wing portion is around 63.8 deg and 38 deg respectively from the horizontal as shown in Fig. 2. The Reynolds number for the investigation has been fixed as 58500 based on the mean aerodynamic chord (MAC). The details pertaining to the experimental setup and computations are discussed in the subsequent sections.

Figure 2a shows a typical overview of the BWB model with different regions highlighted and Fig. 2b shows the dimensional details of the model for simulations. The strake was at an angle of 63.8 deg while the wing was inclined at 38 deg, which was simply based upon the model reported by Qin *et al.* (2004). The BWB model analysed, consisted of different aerofoil sections of which the section of aerofoil at the wing root and the tip are shown in Fig. 3.

2.1. Experimental Setup

All the experiments were conducted in the low-speed Tunnel in Aerodynamics Laboratory at Birla Institute of Technology, Mesra, Ranchi shown in Fig. 4. The low-speed tunnel is an open circuit and has a test section size of 0.6 m x 0.6 m and the freestream velocity ranges from 0 – 30 m/s.

The turbulent intensity measured in the test section with the help of a hotwire anemometer was found to

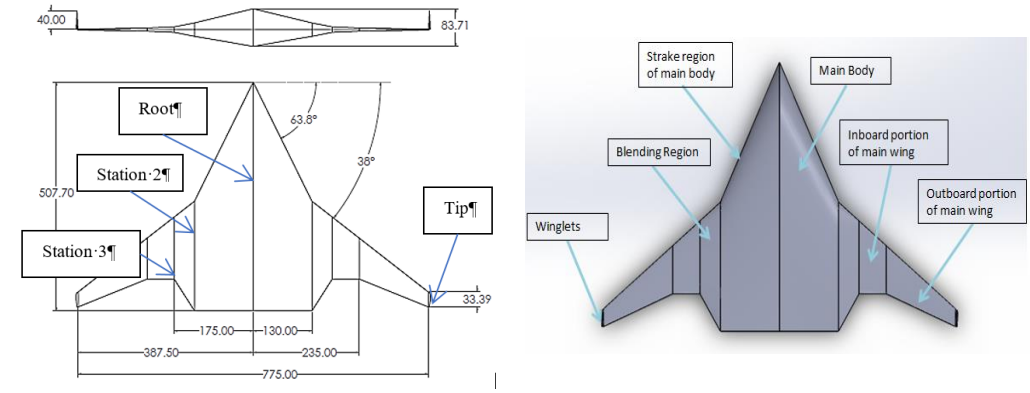

(a) (b)

Fig. 2. (a) Different Regions of BWB model (b) Dimensional details of BWB model (mm).

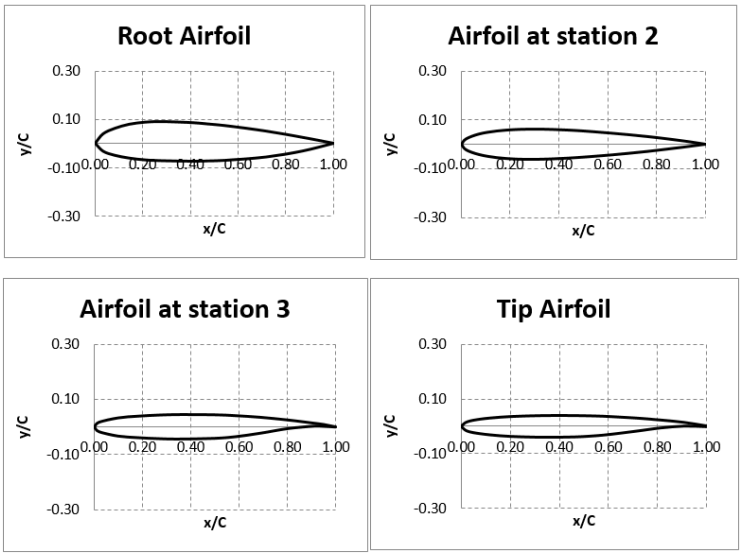

Fig. 3. Airfoil section at different locations of BWB model.

Fig. 4. Low Speed Wind Tunnel.

be better than 0.3%. A BWB model like the one reported in Qin *et al*. (2004) was used in the present investigation. The BWB model was manufactured using a 3D printer (FDM-based) which is shown in Fig. 5. The surface roughness measured indicated a Ra value better than 5.

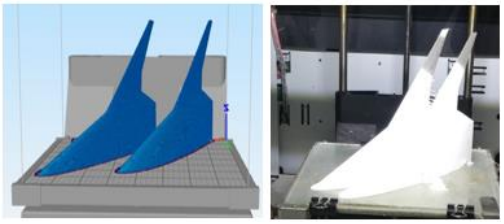

(a) (b)

Fig. 4. (a) Sliced model with split sections. (b) Printed model in 3d printer.

The test model was scaled and had a center chord of 187.85 mm and a span of 286.75 mm. An internal five-component strain gauge balance was used to measure the forces over the model. The strain gauge balance had a diameter of 15 mm and it was suitably mounted on the incidence mechanism for the measurement of forces. The experimental model mounted in the wind tunnel is depicted in Fig. 6. Minimum interference was ensured in the wake region due to the mounting arrangements. A low noise 3 volt DC power supply powered through a isolation transformer was utilized to excite the bridges of the strain gauge balance. A signal conditioner with a 10Hz low pass filter was used to obtain the voltage to improve the signal-to-noise ratio. A sampling rate of 500 Hz was used to obtain steady state measurements. Error of less than 5% was observed during the repeatability tests. A computer-controlled incidence mechanism was used to vary the angle of attack of the model. Minimum/ negligible vibration was ensured during the test run.

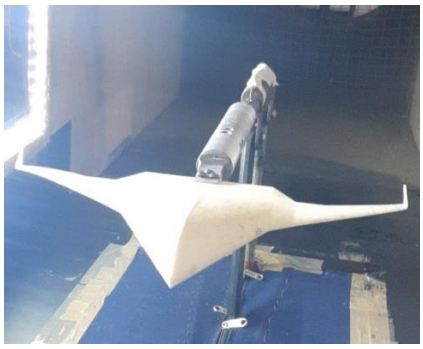

Fig. 6. Experimental model mounted in wind tunnel.

Surface flow visualization was made using the oil flow technique as described in text by Maltby (1962). A typical mixture of carbon soot, oleic acid, and lubricating oil was prepared in suitable proportion and was sprayed on the test model so that the mixture appeared to be tiny droplets/ oil dots on the model surface. The wind tunnel was made to run, and the streak lines were formed from the oil dots. The pattern which appeared was captured with the help of a Digital Single Lens Reflex Camera. The oil flow technique is one of the simplest techniques to identify the separation and attachment zones in a flow.

2.2. Computational Methods

Computational fluid dynamics was carried out on the BWB using the commercial software ANSYS. A three-dimensional, time-dependent, and pressure-based solver was used to compute the flow field over the BWB model. A structured grid was made on the BWB model and the grids were more clustered near the model. The computation model dimensions are shown in Fig. 2(b). The computational model had a mid chord of 507.7 mm and a span of 775 mm. The Reynolds number based on MAC was maintained same as for experiments by maintaining a lower velocity of about 7 m/s for the computational model. A rectangular domain was made (Fig. 7) and the inlet and outlet were placed at a distance of 20 times the mean chord respectively. The surface grid is shown in Fig. 8. A second-order spatial and temporal discretization scheme was employed in the present computational method. A time step of 0.001 second was used for the present computations. Keeping in view, the massive separation at angles of attack, a fully turbulent flow was assumed and hence initially Spalart Allamaras (SA) turbulence model was used in the present computation as it is suitable for the external flows as peer analysis carried out by Kumar and Prasad (2016). Further computations were also carried out using the two equation K-ω SST turbulence model. A grid independence study was carried out using both turbulence models as stated in the following section.

2.3. Grid Independence Study

The results obtained using S-A turbulence model was in better agreement for the lift values with the measured data (Table 1) at low angles of attack and results obtained using K-ω SST turbulence model in better agreement for the drag values with the

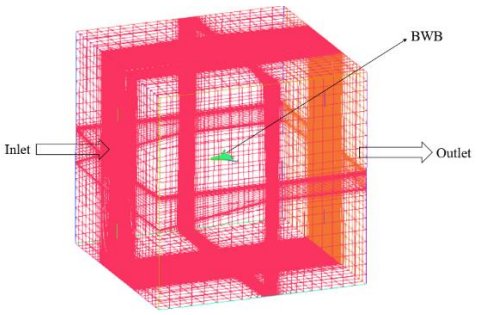

Fig. 7. Computational Domain around BWB.

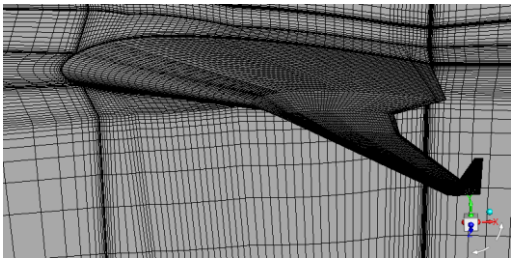

Fig. 8. Grid distribution over BWB surface and center plane.

measured data (Table 1). It was observed that at higher angles of attack, Values obtained from S-A turbulence model deviated from experimental results drastically and hence the results of the computations presented here were carried out using K-ω SST turbulence model.

Suitable boundary conditions such as velocity inlet, outflow, and wall conditions were enforced. Grid independence tests were conducted for three different grid sizes of 1.8 million, 2.25 million, and 2.47 million. Grids were made more clustered near the body surface with the increase in the grid size. For the grid, minimum wall spacing was taken corresponding to y+ around 1. In all these cases, the grids were mainly increased near to the body to capture the flow field. Table 1 shows the effect of grids on the lift and drag coefficients in comparison to the measured values. Apart from this, the effect of turbulence model was also obtained which indicate that K- ω SST turbulence model had a better agreement with the measured values. Hence, K- ω SST turbulence model was utilised for further computations. It has also been reported in several literature that S-A turbulence model is well suited for external flows as well as near wall conditions.

3. RESULT AND DISCUSSION

Flow investigation over a Blended Wing Body was conducted at different angles of attack at low speeds adopting experiments and computational methods. Figure 9 shows the variation of lift coefficient with respect to the angles of attack. A linear increase in the lift coefficient is observed with the increase in the angle of attack up to 15 degrees after which the lift curve slope appears to decrease and at around $\alpha = 35$ deg, it starts to drop indicating stall. The computed lift coefficient for the present case is using K-ω turbulence model. For S-A turbulence model seems to be in better agreement with the measured values for low angles of attack while for higher angles, it appears to deviate and continually predict higher lift than what is achieved in experiments. The K-ω SST model is in close agreement with the experimental results. The drag values shown in Fig. 10 are in close agreement for both K-ω SST and SA model runs with the experiments. Hence the computational result have shown for K- ω SST model only. A trend is observed where the drag increases significantly after 10 degrees angle of attack. A similar trend was observed for the results of computational fluid dynamic analyses made in the angle of attack range of -10 deg to 15 deg reported by Yamada *et al.* (2019), however, differences could be observed at higher angles of attack. Repeatability test indicated a low standard deviation in the mean values. Figure 10 shows the variation of drag coefficients with the angle of attack which indicated an increase in the drag with increasing angles of attack. The measured and computed were in reasonable agreement. The variation of the ratio of lift to drag (L/D) with respect to the angles is shown in Fig. 10 which indicates a better aerodynamic efficiency at lower angles of attack. An interesting comparison between the lift and drag of BWB and double delta wing was carried out which is shown in Fig. 11 and 12 respectively. Figure 13 shows the variation of lift with drag. The comparison indicates that BWB has a clear advantage over the conventional double delta wing used in the present aircraft at low angles of attack with the BWB lift curve slope closely matching the Double Delta wing at higher angles of attack.

To understand the behaviour of the flow over the surface of the blended wing body, oil flow visualization was carried out on the surface of the test model. To the best of the author's knowledge, such visualizations on a Blended Wing Body (BWB) are very limited in the literature. Figure 14a shows the oil flow pattern on the leeward side of the BWB at an angle of attack of 0 deg. The flow seems to be almost attached to the surface of the wing, however, the movement of high momentum fluids over the surface leaves a pattern that appears slightly downstream of the leading edge of the main body and moves towards the wings. The wings experience a fully attached flow which is similar to the case of the flow visualization over a typical aerofoil. The flow however appears to be complicated even at an angle of attack of 0 deg. Figure 14b shows the oil flow visualization at an angle of attack of 5 deg. In comparison to the case of 0 deg, the flow seems to have experienced separation at the leading edge of the outer section of the wing, still, flow over the main body portion seems to be attached. The attached flow

Table 1. Grid independence test and effect of turbulence model (α = 10 deg).

Computation				**Present Experiments**
Grid	***Grid 1***	***Grid 2***	***Grid 3***	
Grid Size (in millions)	1.8	2.25	2.47	
C_L (S-A)	0.826	0.825	0.825	0.826
C_L (K-omega SST)	0.769	0.771	0.771	
C_D (S-A)	0.128	0.127	0.126	0.144
C_D (K-omega SST)	0.132	0.129	0.13	

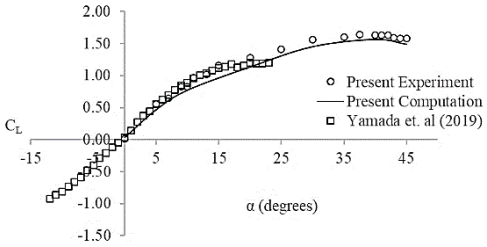

Fig. 9. Comparison of lift at different angles of attack.

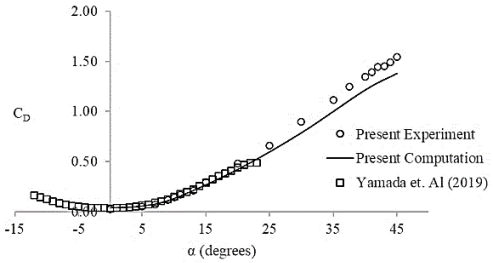

Fig. 10. Comparison of drag at different angles of attack.

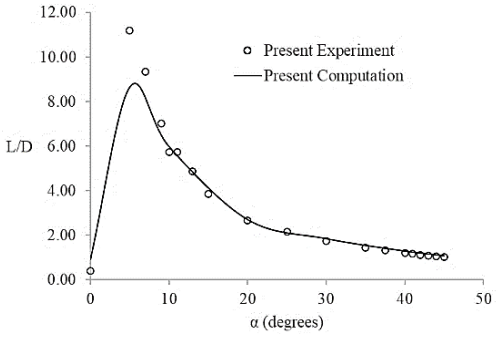

Fig. 11. L/D ratio for different angles of attack.

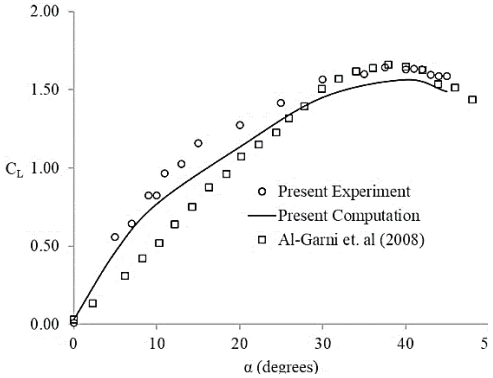

Fig. 12. C_L vs α comparison for present study and double delta wing (Al. Garni *et al*. 2008) for different angles of attack.

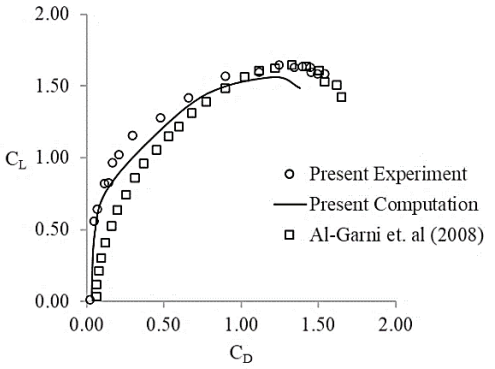

Fig. 13. C_L vs C_D comparison for present study and double delta wing (Al. Garni *et al.* 2008) for different angles of attack.

due to the aerofoil shape of the main body leads to the increase in the lift of the body as observed in the force measurements (Fig. 9). Apart from this the flow over the leading of the wing also seems to interact with the main body flow and a typical separation line pattern is observed in the blending region of the main body and wing. The flow over the BWB appeared more dramatic with a further increase in the angle of attack to 10 deg (Fig. 14c). The attached flow over the main body seems to move inboard over the wings and a typical reversal in the flow is observed in the blending region of the main body and wing. There seemed to be a large interaction between the flow over the wing and main body leading to such a recirculation zone. However, such a complex behaviour of the flow is expected to create a larger suction zone leading to an increasing lift coefficient at 10 deg angle of attack. At an angle of attack of 20 deg (Fig. 14d), it was observed that the wing region of BWB model experienced negligible fluid movement, and hence the oil dots didn't move, while a massive fluid movement is observed on the main body central region. The appearance of separation lines indicates the presence of a strong vortex in the vicinity. The presence of such vortical structures is expected to add to the lift as well as drag coefficient which is observed in Fig. 9 and 10 respectively. With further increase in the angle of attack to 30 deg (Fig. 14e), the vortices seem to leave the surface and burst. With further increase in the angle of attack to 40 deg and 50 deg (Fig. 14f and 14g), the vortices lifting seems to move upstream which is expected to reduce the lift and augment the drag (Fig. 9 and 10). The overall oil flow visualization indicated no major asymmetrical pattern on the surface.

To get more insight into the flow, computational fluid dynamics were carried out on the BWB model. Three-dimensional analyses were performed with the help of an unsteady Reynolds Averaged Navier Stokes equation combined with the one equation S-A turbulence model and another set of analysis with k-w SST model. The contour plots for the comparison were taken from the analysis with K-w SST model. Figure 15a shows the comparison of the computational and experimental oil flow pattern carried out on the BWB which indicates a reasonably good agreement. At an angle of attack of 5 deg (Fig.

15b), the appearance of the separation line in the experimental oil flow could also be observed in the case of computational oil flow. This is mainly due to the separation on the aerofoil section of the wing. Interestingly, the complicated flow feature observed in the case of BWB at $\alpha = 10$ deg in the experiment was also observed in the case of computational analyses (Fig. 15c). The feature of flow reversal at the blending junction was observed in both experiments and computational analyses. At an angle of attack of 20 deg (Fig. 15d), a clear interaction of the main body attached flow and leading-edge vortices seemed to appear, which is likely the reason for the reversal of flow in the zone of the wing and main body blending. It is to be noted that the main body flow seems to be more dominant at higher angles of attack. Computed oil flow at $\alpha = 30$ deg and 40 deg seemed to be in reasonable agreement with the experiments (Fig. 15e and 15f). To support the oil flow visualization, the computed skin friction coefficient was extracted and is shown in Fig. 16. Oil mixture gets washed away in the region with a higher value of skin friction, while remains negligibly disturbed in the region of separation (Maltby 1962).

The contour of the vorticity magnitude was plotted at different cross planes of the BWB. Figure 17a shows the vorticity magnitude contour at an angle of attack of 0 deg. No dominant vortices were observed at $\alpha = 0$ deg. Similar features were observed with an increase in the angle of attack to 5 deg (Fig. 17b) wherein a underdeveloped vortex was observed and

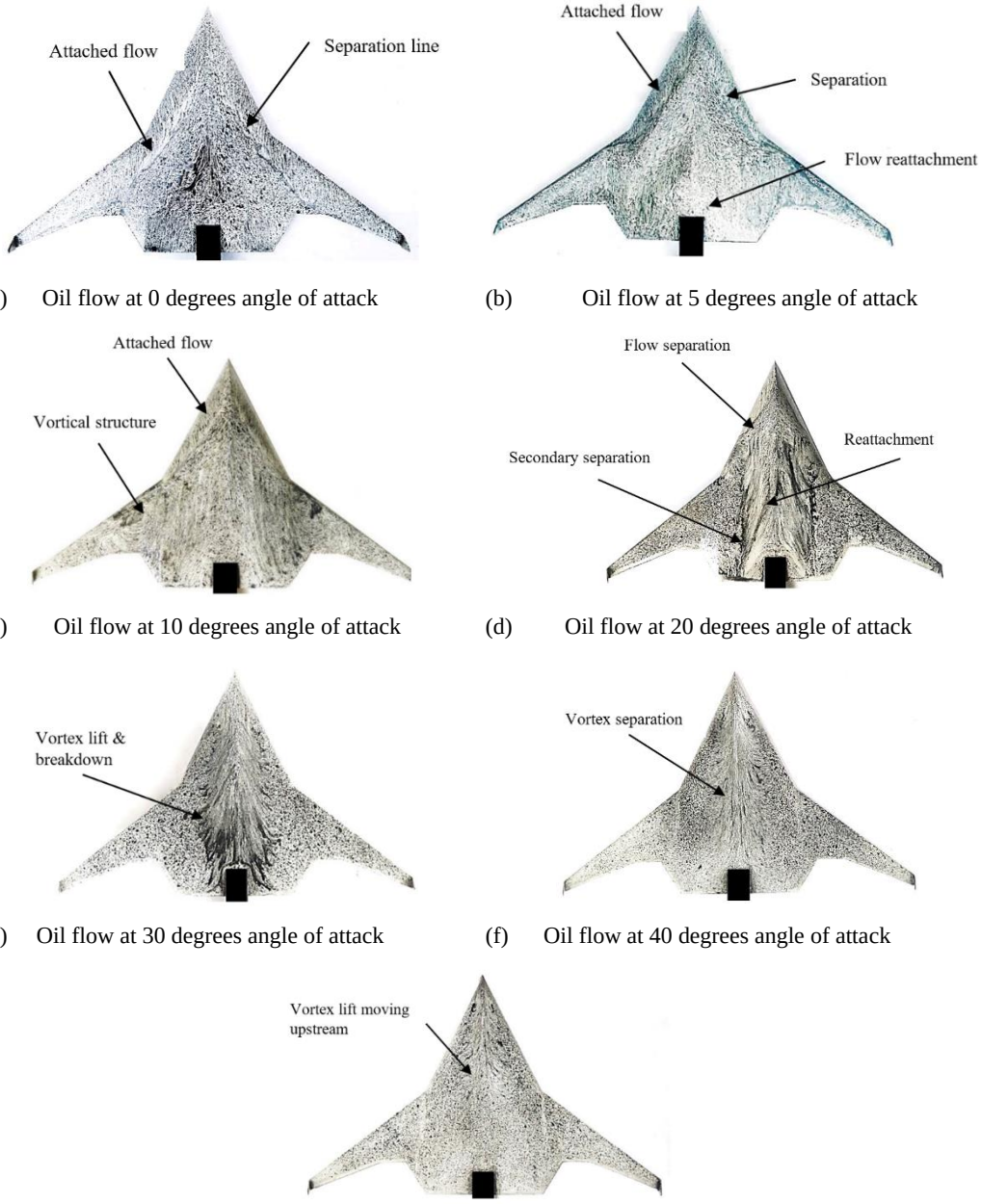

(a) Oil flow at 0 degrees angle of attack

(b) Oil flow at 5 degrees angle of attack

(c) Oil flow at 10 degrees angle of attack

(d) Oil flow at 20 degrees angle of attack

(e) Oil flow at 30 degrees angle of attack

(f) Oil flow at 40 degrees angle of attack

(g) Oil flow at 50 degrees angle of attack

Fig. 14. Comprehensive Caption: Oil flow results at different AoA.

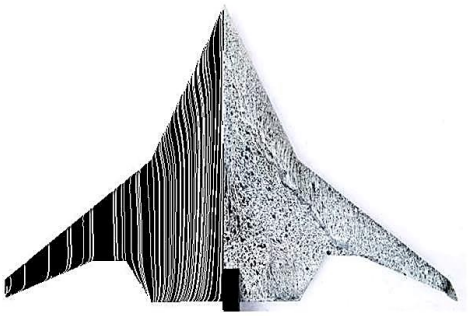

(a) Oil flow over BWB model compared with streamline contour from computation at 0^0 AoA

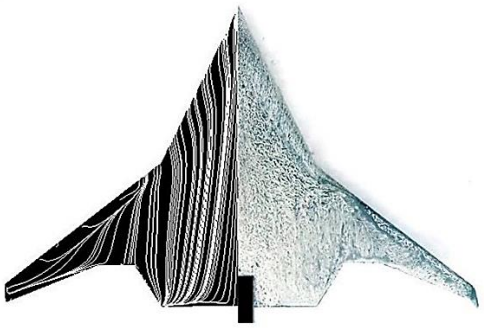

(b) Oil flow over BWB model compared with streamline contour from computation at 5^0 AoA

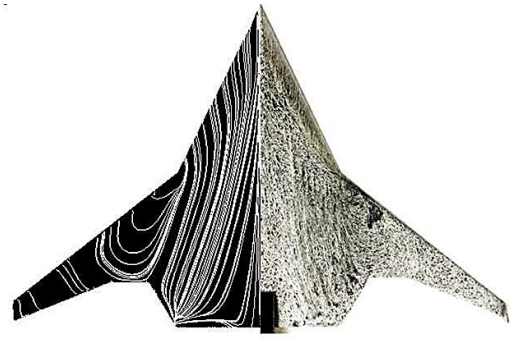

(c) Oil flow over BWB model compared with streamline contour from computation at 10^0 AoA

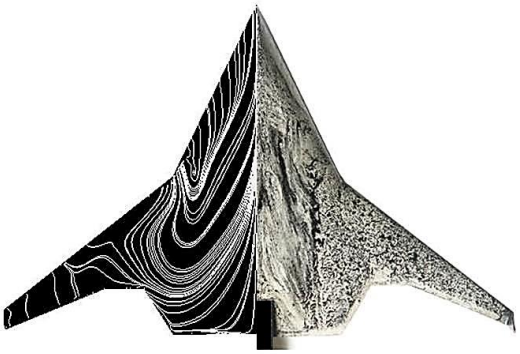

(d) Oil flow over BWB model compared with streamline contour from computation at 20^0 AoA

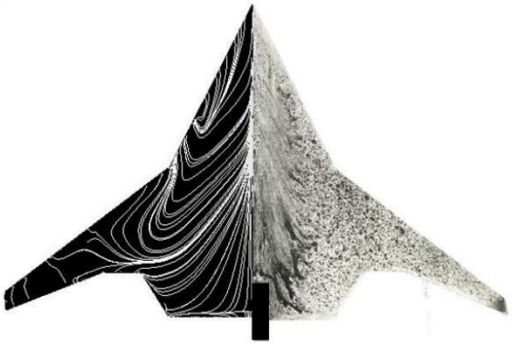

(e) Oil flow over BWB model compared with streamline contour from computation at 30^0 AoA

(f) Oil flow over BWB model compared with streamline contour from computation at 40^0 AoA

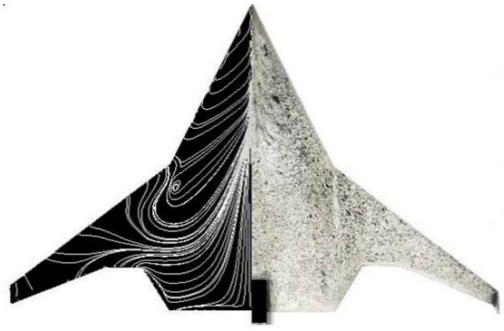

(g) Oil flow over BWB model compared with streamline contour from computation at 50^0 AoA

Fig. 15. Comparison of experimental oil flow and CFD streamlines at different AoA

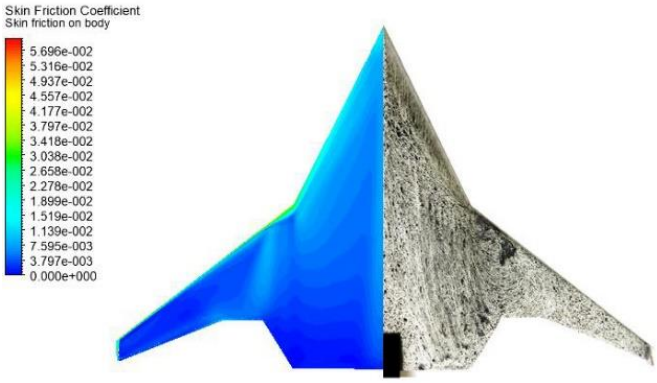

Fig. 16. Oil flow over BWB model compared with skin friction contour from computation at 10^0 AoA.

the whole BWB was dominant by flow features similar to the case of the aerofoil. With further increase in the angle of attack to 10 deg (Fig. 17c), leading-edge vortices similar to the vortices observed in the case of a double delta wing seemed to appear. The existence of such a high-energy rotating fluid system is expected to attract the main body fluid towards itself (Refer Fig. 17c). This leads to a reversal in the flow which was observed in the region where the leading-edge vortex and main body flow interacts. The region happens to be the blending zone of the wing and main body. With further increase in the angle of attack, the flow behaved more like the one over the delta wing wherein two strong counter-rotating vortices were observed which led to the augmentation of lift as well as drag (Fig. 9 and 10). At angles of attack beyond 30 deg (Fig. 17e to 17g), the counter-rotating vortices leave the surface which further leads to the stall of the wing at an angle of attack at 40 deg.

The investigations performed indicated the advantage of BWB configuration in comparison to the conventional tube and wing and the double delta wing configurations. A more detailed analysis of the flow over a Blended Wing Body is required for a better understanding of flow physics.

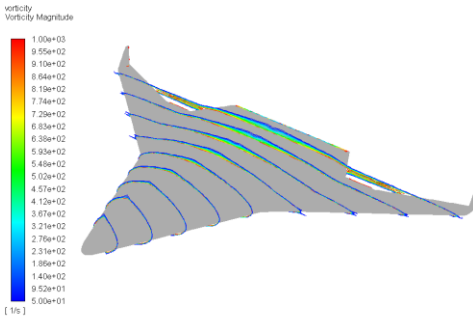

(a) Vorticity over BWB model from computation at 0^0 AoA.

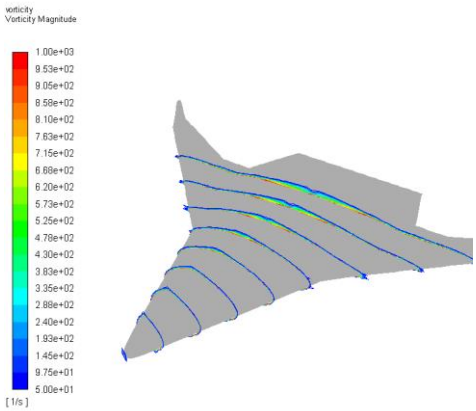

(b) Vorticity over BWB model from computation at 5^0 AoA

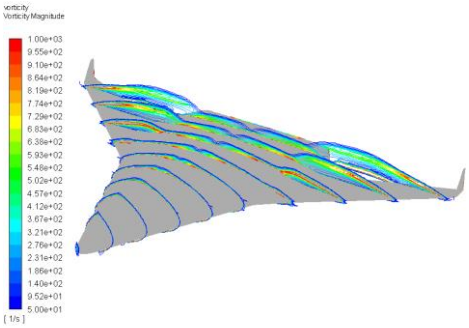

(c) Vorticity over BWB model from computation at 10^0 AoA

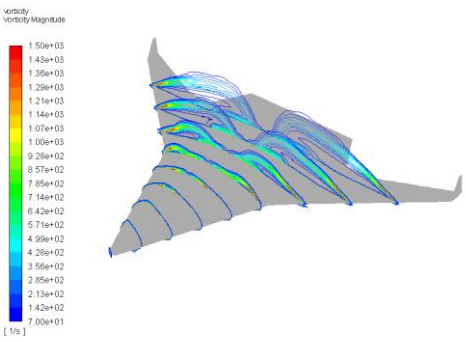

(d) Vorticity over BWB model from computation at 20^0 AoA

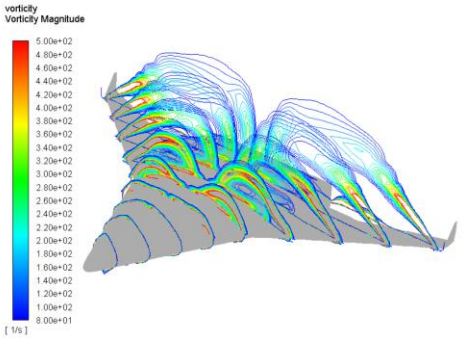

(e) Vorticity over BWB model from computation at 30^0 AoA

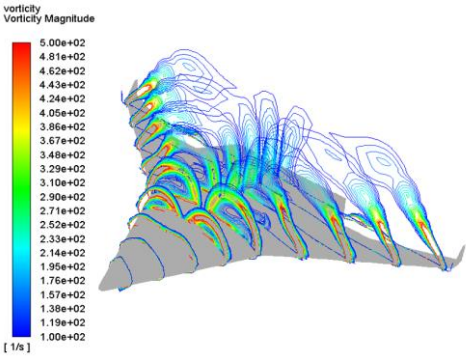

(f) Vorticity over BWB model from computation at 40^0 AoA

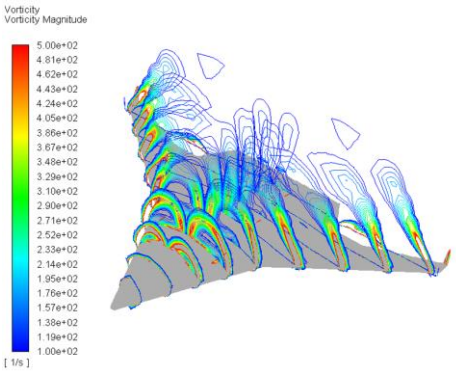

(g) Vorticity over BWB model from computation at 45^0 AoA

Fig. 17. Vorticity contours at different AoA

4. Conclusion

Experiments were conducted over a Blended Wing Body at a Reynolds number of 58500 based on the mean aerodynamic chord and free stream velocity of 19 m/s for experiments. Computations were conducted for the same Reynolds number based on the mean aerodynamic chord. Results indicated an

increase in the lift and drag of the BWB with increasing angle of attacks. The performance seemed to be better than the case of a double delta wing at lower angles of attack, however, further detailed analysis is required for a conclusive comparison. The lift to drag ratio was found to be maximum at an angle of attack of around 5 deg. Surface flow visualization indicated the existence of a highly complex flow pattern on the BWB. At lower angles of attack, the flow was dominated by the attached flow and the lift generated is mainly due to the pressure difference generated because of the cambered shape and the separated flow leading to the counter rotating vortices. At higher angles of attack, the counter-rotating leading-edge vortices become more dominant, and the flow appears similar to the case of a double delta wing. A highly complicated flow behaviour was observed at higher angles of attack at the junction of the fuselage and wings. Computational analyses made on the BWB revealed more details of the flow and the results were found to be in reasonable agreement with the experiments.

References

Al-Garni, A. Z., F. Saeed and A. M. Al-Garni (2008). Experimental and numerical investigation of 65 degree Delta and 65/40 degree double-delta wings. *Journal of Aircraft* 45(1), 71-76.

Becker, M. and D. Sheffler (2016). Designing a high speed, stealthy, and payload-focused VTOL UAV. In *IEEE Systems and Information Engineering Design Symposium (SIEDS)*, Charlottesville, VA, USA.

Brown, M. and R. Vos (2018, January). Conceptual Design and Evaluation of Blended-Wing-Body Aircraft. In *AIAA SciTech Forum, AIAA Aerospace Sciences Meeting*, Kissimmee, Florida.

Dommelen, V. J. and V. Roelof (2014). Conceptual design and analysis of blended-wing-body aircraft. *Proceedings of the Institution of Mechanical Engineers, Part G: Journal of Aerospace Engineering* 228(13), 2452-2474.

Footohi, P., A. Bouskela and S. Shkarayev (2019, January). Aerodynamic Design of Long-Range VTOL UAV. In *AIAA Scitech Forum*, San Diego, California.

Hileman, J., Z. Spakovszky, M. Drela and M. Sargeant (2007, January). Airframe Design for

Silent Aircraft. In *45th AIAA Aerospace Sciences Meeting and Exhibit*, Reno, Nevada.

Kashitani, M., Y. Suganuma, H. Date, S. Nakao, Y. Takita and Y. Yamaguchi (January, 2015) Experimental study on aerodynamic characteristics of blended-wing-body by a wake integration method. In *53rd AIAA Aerospace Sciences Meeting*, Kissimmee, Florida.

Kumar, P. and J. K. Prasad (2016). Mechanism of Side Force Generation and Its Alleviation over a Slender Body. *Journal of Spacecraft & Rockets* 53(1), 195-208.

Kuntawala, N., J. Hicken and D. Zingg (2011, January). Preliminary aerodynamic shape optimization of a blended-wing-body aircraft configuration. In *49th AIAA Aerospace Sciences Meeting including the New Horizons Forum and Aerospace Exposition*, Orlando, Florida.

Larkin, G. and G. Coates (2017). A design analysis of vertical stabilisers for Blended Wing Body aircraft. *Aerospace Science and Technology* 64, 237-252.

Lehmkuehler, K., K. Wong and D. Verstraete (2012, September). Design and test of a UAV blended wing body configuration. In *Proceedings of the 28th Congress of the International Council of the Aeronautical Sciences*, ICAS.

Liebeck, R. H. (2003, July). Blended Wing Body Design Challenges. In *AIAA/ICAS International Air and Space Symposium and Exposition: The Next 100 Y*, Dayton, Ohio.

Liebeck, R. H. (2004). Design of the Blended Wing Body Subsonic Transport. *Journal of Aircraft* 41(1), 10-25.

Lyu, Z. and J. R. Martins (2013a). RANS-based aerodynamic shape optimization of a blended-wing-body aircraft. In *21st AIAA Computational Fluid Dynamics Conference*, San Diego.

Lyu, Z. and J. R. Martins (2013b, January). Aerodynamic shape optimization of a blended-wing-body aircraft. In *51st AIAA Aerospace Sciences Meeting including the New Horizons Forum and Aerospace Exposition*, Grapevine (Dallas/Ft. Worth Region), Texas.

Maltby, R. L. (1962, April). *Flow Visualization in Wind Tunnels Using Indicators.* Advisory Group for Aeronautical Research and Development Paris (France).

Midhun, M. V., P. Mondal, P. K. Karn and P. Kumar (2019, August). Numerical and Experimental Investigation of Blended Wing Body Configuration. In *21st Annual CFD Symposium*, Bangalore.

Naeini, H. K., M. Nili-Ahmadabadi and K. C. Kim (2019). An experimental study on the effect of a novel nature-inspired 3D-serrated leading edge on the aerodynamic performance of a double delta wing in the transitional flow regime. *Journal of Mechanical Science and Technology* 33(12), 5913-5921.

Naeini, H. K., M. Nili-Ahmadabadi, Y. S. Park and K. C. Kim (2021). Effect of nature-inspired needle-shaped vortex generators on the aerodynamic features of a double-delta wing. *International Journal of Mechanical Sciences* 202, 106502.

Panagiotou, P. and K. Yakinthos (2017, June). Parametric aerodynamic study of Blended-Wing-Body platforms at low subsonic speeds for UAV applications. In *AIAA AVIATION Forum, 35th AIAA Applied Aerodynamics Conference*, Denver, Colorado.

Panagiotou, P., S. Fotiadis-Karras and K. Yakinthos (2018). Conceptual design of a blended wing body MALE UAV. *Aerospace Science and Technology* 73, 32-47.

Qin, N., A. Vavalle, A. L. Moigne, M. Laban, K. Hackett and P. Weinerfelt (2002, September). Aerodynamic studies for blended wing body aircraft. In *9th AIAA/ISSMO Symposium on Multidisciplinary Analysis and Optimization*, Atlanta, Georgia.

Qin, N., A.Vavalle, A. L. Moigne, M. Laban, K. Hackett and P. Weinerfelt (2004). Aerodynamic considerations of blended wing body aircraft. *Progress in Aerospace Sciences* 40, 321-343.

Rodzewicz, M., Z. Goraj and A. Tomaszewski (2018). Design and testing of three tailless unmanned aerial vehicle configurations built for surveillance in Antarctic environment. *Proceedings of the Institution of Mechanical Engineers, Part G: Journal of Aerospace Engineering* 232(14), 2598-2614.

Siouris, S. and N. Qin (2007). Study of the Effects of Wing Sweep on the Aerodynamic Performance of a Blended Wing Body Aircraft. *Proceedings of the Institution of Mechanical Engineers, Part G: Journal of Aerospace Engineering* 221(1), 47-55.

Thompson, D., J. Feys, M. Filewich, S. Abdel-Magid, D. Dalli and F. Goto (2011, January). The design and construction of a blended wing body UAV. In *49th AIAA Aerospace Sciences Meeting Including the New Horizons Forum and Aerospace Exposition*, Orlando, Florida.

Yamada, T., M. Taguchi, N. T. Duong, M. Kashitani, K. Kusunose and Y. Takita (2019). Wake Measurements on Blended Wing Body with Gurney Flaps in Low Speed Flows. In *AIAA Scitech 2019 Forum*, San Diego, California.

Zeng, C., R. Abnous and S. Chowdhury (2017). Aerodynamic modeling and optimization of a blended-wing-body transitioning uav. In *18th AIAA/ISSMO Multidisciplinary Analysis and Optimization Conference*, Denver, Colorado.